Contents lists available at ScienceDirect

Soil Biology and Biochemistry

journal homepage: http://ees.elsevier.com

Holm oak decline and mortality exacerbates drought effects on soil biogeochemical cycling and soil microbial communities across a climatic gradient

D. García-Angulo [a], A.-M. Hereş [a,b], M. Fernández-López [c], O. Flores [d], M.J. Sanz [a,e], A. Rey [d], F. Valladares [d,f], J. Curiel Yuste [a,e,*]

[a] BC3 - Basque Centre for Climate Change, Scientific Campus of the University of the Basque Country, 48940, Leioa, Spain
[b] Department of Forest Sciences, Transilvania University of Braşov, Şirul Beethoven -1, 500123, Braşov, Romania
[c] Estación Experimental del Zaidín (EEZ, CSIC), Calle Profesor Albareda 1, 18008, Granada, Spain
[d] LINCGlobal, Museo Nacional de Ciencias Naturales (MNCN-CSIC), Serrano 115, 28006, Madrid, Spain
[e] IKERBASQUE - Basque Foundation for Science, Maria Diaz de Haro 3, 6 solairua, 48013, Bilbao, Bizkaia, Spain
[f] Universidad Rey Juan Carlos, Dpto. Biología y Geología, Física y Química Inorgánica, Calle Tulipan s/n, Mostoles, 28933, Madrid, Spain

ARTICLE INFO

Keywords
Drought-induced mortality
Holm oak
Nitrogen mineralization
Nitrifiers
Ectomycorrhizal fungi (ECM)
Cascading effects

ABSTRACT

The extent to which the increasingly frequent episodes of drought-induced tree decline and mortality could alter key soil biogeochemical cycles is unclear. Understanding this connection between tree decline and mortality and soils is important because forested ecosystems serve as important long-term sinks for carbon (C) and essential nutrients (e.g., nitrogen and phosphorus). In order to fill in this knowledge gap, we conducted a study on 13 sites distributed across the Spanish Iberian Peninsula where the dominant tree species was the Mediterranean evergreen Holm oak (*Quercus ilex* L. subsp. *ballota* [Desf.] Samp), a species that has shown important drought-induced crown defoliation and mortality rates in recent decades. Our study covered different climatic, soil, land-use type (forests, dehesas, and open woodlands), and crown defoliation (healthy, affected, and dead Holm oaks) gradients that characterize this species distribution within the Spanish Iberian Peninsula. Specifically, the soil C and nutrient content (nitrogen, N; phosphorus, P; magnesium, Mg), several functional parameters (heterotrophic respiration (R_H); N mineralization (i.e., N ammonification, R_{amm}; and N nitrification, R_{nit})), and relative abundances of key microbial soil functional groups (nitrifiers and ectomycorrhizal fungi (ECM)) were studied. Our results showed that aside from the potential effects associated with the climatic gradient, Holm oak decline and mortality resulted in soil stoichiometric imbalances triggered by net losses of essential oligonutrients (e.g., Mg) and the accumulation of very mobile forms of nitrogen (NO_3^- - N) and available phosphorus (Av P). Changes in the abundance of key microbial soil functional groups (nitrifiers and ECM) co-occurred with observed nitrate and available P accumulation. Therefore, we conclude that the potential vulnerability of soil C and nutrient stocks to ongoing changes in climate may strongly depend on tree vulnerability to climate change, its effect on soil-plant relationships, and how this may impact the ecology and functioning of key soil functional groups and key metabolic pathways.

1. Introduction

It is expected that increases in the severity and intensity of drought events, associated with climate change, will have an enormous impact on soil biogeochemical cycling (Schlesinger et al., 2016). This is, as many studies have shown, because soil biota (Curiel Yuste et al., 2014; Valencia et al., 2018; Moreno-Jiménez et al., 2019) and soil functioning (Curiel Yuste et al., 2007; Chen et al., 2011; Moyano et al., 2012) are extremely sensitive to changes in water availability, which subsequently impacts the cycling of C and nutrients in soils (Sardans and Peñuelas, 2005; Xu et al., 2016; Curiel Yuste et al., 2017). In the particular case of Mediterranean ecosystems, where soil moisture plays a critical role in plant growth and soil activity (Vilà and Sardans, 1999; Sardans and Peñuelas, 2005; Casals et al., 2009), both the duration of drought events (e.g., Ma et al., 2012; Vargas et al., 2018) and the cycles of drying and rewetting, to which soils are submitted to (e.g., Barnard et al., 2013; Rodríguez et al., 2019), have been identified as drivers of change in rates of soil biogeochemical cycling.

* Corresponding author. BC3 - Basque Centre for Climate Change, Scientific Campus of the University of the Basque Country, 48940, Leioa, Spain.
E-mail address: jorge.curiel@bc3research.org (J. Curiel Yuste)

https://doi.org/10.1016/j.soilbio.2020.107921
Received 6 November 2019; Received in revised form 8 July 2020; Accepted 9 July 2020
Available online xxx
0038-0717/

So far, studies and models have generally omitted other potentially important impacts of the observed increases in the frequency and intensity of drought on the soil ecosystem. Specifically, the extent to which drought-associated tree decline and mortality events (Allen et al., 2010, 2015; Hartmann et al., 2018), in some cases overlapping with pathogen outbreaks (Edburg et al., 2012; Corcobado et al., 2014), are affecting the functioning of the soil ecosystem are still unknown (Anderegg et al., 2012; McDowell et al., 2018). This knowledge gap is of particular relevance since tree decline and mortality has become a worrisome phenomenon now affecting ecosystem forests all over the world (Allen et al., 2010, 2015; Hartmann et al., 2018) and climate change models forecast more frequent and intense drought events (IPCC, 2014; Mariotti et al., 2015), which will probably determine more tree decline and mortality events. However, there are still many uncertainties about the extent to which tree decline and mortality could affect the functioning of soils and their ability to sequester C and nutrients (Schlesinger et al., 2016). Soil microbial communities and nutrient cycling related functions are very sensitive to changes in microclimatic conditions (Sardans and Peñuelas, 2005, Curiel Yuste et al., 2007; Curiel Yuste et al., 2017). Thus, alterations of the soil microclimatic conditions associated with crown defoliation, due to decreases in transpiration or canopy interception of precipitation and solar radiation (Anderegg et al., 2012), may severely affect soil functioning and soil biogeochemical cycling. Furthermore, the modification of the belowground carbon (C) flow resulted from the interruption of exudation (Högberg et al., 2001) and/or the increased input of litterfall and dead wood (Curiel Yuste et al., 2019), may also alter nutrient and C cycling (Avila et al., 2016; Rodríguez et al., 2017; Flores-Rentería et al., 2018) and the composition of key microbial soil functional groups (Curiel Yuste et al., 2012; Lloret et al., 2015). The cycling of nitrogen (N) in soil, which is particularly sensitive to changes in soil moisture (Chen et al., 2011; Xu et al., 2016; Curiel Yuste et al., 2019), might be also sensitive to the microclimatic alterations associated with tree decline and mortality. For instance, Rodríguez et al. (2017), found a significant increase in N mineralization due to drought-induced Holm oak decline and mortality. In fact, Holm oak decline may increase the response of N mineralization during drying-rewetting cycles (Rodríguez et al., 2019) suggesting that tree decline and mortality may accelerate N mineralization under infrequent rains. The accumulation of more mobile forms of N (e.g., nitrate, NH_3^--N), resulted from its increased mineralization (Rodríguez et al., 2017, 2019; Avila et al., 2019), could result in net losses of N from the system because NO_3^- - N is susceptible of being leached out of the system. However, to the best of our knowledge, no studies have yet explored in detail how drought-induced tree decline (i.e., estimated using crown defoliation; see below) and mortality could affect microbial N cycling-related functional groups and N cycling at larger regional scales.

In this study, we investigated the potential effects of Holm oak (*Quercus ilex* L. subsp. *ballota* [Desf.] Samp) decline and mortality on soil biogeochemical cycling, soil microbial C and N mineralization, and key soil functional groups (nitrifiers and ectomycorrhizal fungi, ECM) within the Spanish Iberian Peninsula. Specifically, our main aim was to understand how Holm oak decline and mortality may be an agent of change that accelerates or exacerbates the effects of climate change on soil biogeochemical cycling, soil microbial C and N mineralization, and key soil functional groups. For this, we worked with 13 Holm oak study sites distributed along the Spanish Iberian Peninsula covering as uniform as possible different climatic, soil, land-use type (forests, dehesas, and open woodlands), and crown defoliation (healthy, affected, and dead Holm oaks) gradients that characterize this species distribution. Although Holm oak is a Mediterranean species considered to be well adapted to drought conditions, it has undergone significant drought-related decline and mortality rates in recent decades (Lloret et al., 2004; de Sampaio e Paiva Camilo-Alves et al., 2013; Hereş et al., 2018). We used these 13 Holm oak sites to study potential effects of climate and defoliation over soil pools, functions and functional groups related to the cycling of C, N, and P, and essential oligonutrient content (e.g., magnesium or potassium). We hypothesize that: i) the impact of drought-associated Holm oak decline and mortality on soil biogeochemical cycling, soil microbial C and N mineralization, and key soil functional groups (i.e., nitrifiers and ECM) may obscure or even exacerbate those effects from climate; ii) Holm oak decline and mortality could alter concentrations of mineral N in soils because tree decline and mortality may affect soil key functional groups responsible for the consumption (ECM) and generation (nitrifiers) of mineral forms of N.

2. Materials and methods

2.1. Study sites and climatic data

We used a total of 13 Holm oak study sites, all located in the Spanish Iberian Peninsula (Table 1, Fig. 1). Prior to any field visits being made, study sites were selected based on literature (Lloret et al., 2004, Camarero et al., 2016; Corcobado et al., 2014, Camarero et al., 2015), different forest inventories (i.e., the third National Forest

Table 1
Site description including: land-use type (FR, forests; DH, dehesas; OW, open woodland), geographic coordinates (latitude and longitude), elevation, percentage of crown coverage (Cc) per ha, and abiotic factors (MAT, mean annual temperature; MAP, mean annual precipitation; and pH).

Study sites (number)	Land-use type	Latitude	Longitude	Elevation (m)	% Cc (ha $^{-1}$)	MAT (ºC)	MAP (mm)	Soil pH
Huelva (1)	DH	37.9820	−6.5125	405	16	16.15	892	5.89
Tres Cantos (2)	DH	40.6714	−3.6827	806	15	12.86	591	5.54
Chapinería (3)	DH	40.3833	−4.1938	649	27	12.88	601	6.35
Plasencia (4)	DH	39.8775	−6.0490	367	10	15.37	740	5.38
Talavera de la Reina (5)	OW	39.7846	−5.0742	427	47	15.41	559	5.87
Sevilla (6)	OW	37.9727	−6.0193	729	45	15.15	637	6.04
Pamplona (7)	OW	42.7323	−1.7504	624	48	10.62	919	7.33
Formiche Bajo (8)	OW	40.2974	−0.8727	1044	43	13.08	497	7.78
Granada (9)	OW	37.5012	−2.5042	1221	42	12.41	326	7.03
Lleida (10)	FR	41.8304	1.4516	609	63	13.08	569	7.19
Ciudad Real (11)	FR	38.5056	−3.2480	814	85	14.52	484	6.29
Guadalajara (12)	FR	40.8753	−3.1626	889	84	12.10	573	4.86
Alcoy (13)	FR	38.6659	−0.5395	1014	90	13.83	519	7.52

Where, numbers in brackets from column *Study sites (number)* represent the numbers that have been used in Fig. 1 to identify the 13 study sites; pH, mean pH values of all soil samples extracted from each study site.

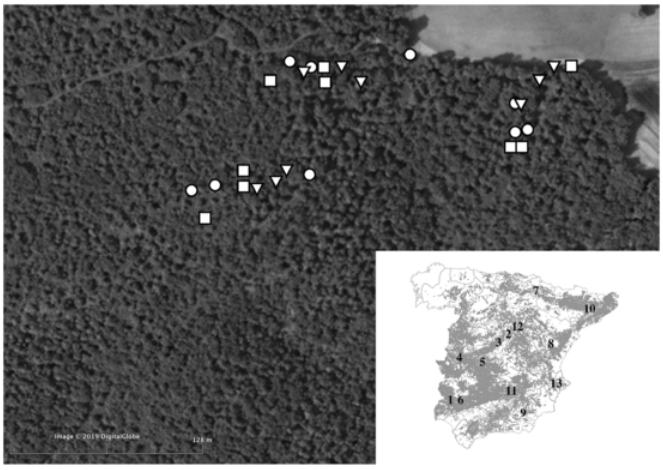

Fig. 1. Holm oak distribution within the Spanish Iberian Peninsula and location of the 13 study sites (inset map). The numbers on the map correspond to the study sites mentioned in Table 1. The satellite image illustrates the sampling design with the 3 subplots that were selected for each of our study sites and the healthy (squares), affected (triangles), and dead (circles) Holm oaks that have been selected and sampled (cf. Materials and methods for details). This satellite image illustrates only one of the 13 sites, as an example, but it is representative for all of them.

Inventory, IFN3; MAGRAMA, 2007), and the International Co-operative Programme on Assessment and Monitoring of Air Pollution Effects on Forests - ICP Forests (http://icp-forests.net/). Site selection aimed to cover as uniformly as possible different aspects of this species distribution within the Spanish Iberian Peninsula: i). climatic and soil pH gradients that characterize its distribution area; and ii). representative land-use types (i.e., forests, dehesas, and open woodlands; see below) (Table 1, Fig. 1). Additionally, all 13 study sites were characterized by high Holm oak decline (e.g., high crown defoliation rates) and drought-induced mortality rates registered in recent decades (Gazol et al., personal communication).

The climate of the 13 study sites varied from oceanic (Cfb; Northern Cantabrian coast, Navarra) to semiarid (BSh; Southwest Mediterranean coast, Alicante), being in most cases continental Mediterranean (Csa; i.e., characterized by hot and dry summers, and rainfall periods mainly concentrated in spring and autumn) according to the Köppen-Geiger map on climate classification (https://es.climate-data.org/europe/espana-5/). The mean annual temperature (MAT) of our study sites varied from 10.62 to 16.15 °C, while their mean annual precipitation (MAP) varied from 326 to 919 mm (Felicísimo et al., 2011, Table 1). MAT and MAP datasets for each of our 13 study sites were obtained from Felicísimo et al. (2011). These climatic datasets had a 1 km resolution grid, covered a period of 57 years (from 1950 to 2007), and were built and validated using climatic data from local meteorological stations (Felicísimo et al., 2011). We decided to use these climatic datasets as our study sites were generally located far from any meteorological station and the modelled MAT and MAP datasets from Felicísimo et al. (2011) were much more precise given that they represent corrected data (i.e., considering elevation gradients).

In order to characterize the 13 study sites depending on their land-use type we used orthophotos, which allowed us to quantitatively estimate the crown coverage of each of the sites (i.e., % of trees per ha; MAGRAMA, 2007). To do so, the SigPac viewer was used (http://signa.ign.es/signa/Pege.aspx). Based on this approach, the following Holm oak land-use types were considered for this study: forests (hereinafter referred to as FR), sites with >60% of crown coverage per ha; dehesas (hereinafter referred to as DH), sites with <30% crown coverage per ha; and open woodlands (hereinafter referred to as OW), sites with 30%–60% crown coverage per ha. In total, 4 FR, 4 DH, and 5 OW were used in this study. The current structure of these three land-use types has been traditionally determined depending on their use. Accordingly, FR have been historically subjected to a low human land-use pressure as they have been mainly used for firewood and hunting. DH instead have been historically subjected to an intense human land-use pressure as they have been transformed into savannah-like ecosystems and used for livestock rearing and grazing, and agriculture (Pulido et al., 2010). Finally, the OW represent abandoned dehesas, meaning that they have been used in the past for livestock rearing and grazing, and agriculture, but are currently not in use (Herguido Sevillano et al., 2017).

2.2. Experimental design and trees characterization

In order to understand the impact of Holm oak decline and mortality on soil biogeochemical cycling, microbial C and N mineralization, and key soil functional groups (ECM and nitrifiers), a factorial experimental design was used. A total of 351 Holm oaks (i.e., 27 trees per site) were selected based on their crown defoliation (i.e., % of foliage lost). Crown defoliation was visually evaluated at the whole tree level and was always estimated by the same observer for consistency. To do so, at each site, one healthy reference Holm oak (i.e., with no signs of crown defoliation) was identified. Then, the 27 Holm oaks per site were compared with this reference trees and classified depending on their percentage of foliage lost (Dobbertin, 2006). Accordingly, at each site, 9 healthy (crown defoliation between 0 and 25%), 9 affected (crown defoliation between 25 and 99%), and 9 dead Holm oaks (crown defoliation of 100%, and no visible signs of re-sprouting) were selected. In order to cover as uniformly as possible the area of each study site and to account thus for within-site heterogeneity (Medina et al., 2015), for each of the 13 study sites, three different subplots were considered. These subplots were established starting from three centroids (i.e., central points) with homogeneous environmental characteristics (i.e., slope, soil exposition), around which all the needed Holm oaks were sampled. Specifically, within each subplot, 9 Holm oak trees (3 healthy, 3 affected, and 3 dead; Fig. S1) were sampled. The objective of this space-for-time substitution design was to study potential effects of defoliation on pools and rate functions by randomizing the error associated with potential microenvironmental differences that could be associated with the crown defoliation condition of the selected Holm oaks. By doing so, the effect of potential confounding factors on the selected Holm oaks was minimized, assuming that the observed variability in crown defoliation (i.e., healthy, affected, and dead trees) could only be attributed to differences in individual tree physiological resilience responses to drought.

For each of the 351 Holm oaks selected for this study, we measured their height using a clinometer, and their diameter at breast height (dbh) using a dbh tape. Additionally, two canopy diameters (i.e., the longest and the shortest) were measured using a tape. These latter measurements were used to calculate the canopy area, using the ellipse area equation. In order to estimate the vegetation area index (VAI), three different hemispheric photographs were taken for each sampled Holm oak tree at 0.5 m above the ground, as close as possible to the trunk. By doing so, we captured the whole surface of their crowns. The hemispheric photographs were taken using a 360° fisheye lens (FCE8, Nikon) and a horizontally-levelled high resolution digital camera (CoolPix 995, Nikon, Tokio, Japan) mounted on a tripod. All these hemispheric photographs were further analyzed using the Hemiview v.2.1 software (Delta-T Devices Ltd, Burwell, UK) and VAI values were separately estimated for each Holm oak.

Finally, around each of the 351 Holm oaks, the percentage of non-herbaceous (shrubs and seedlings), herbs, and bare soil (non-vegetation) cover were visually estimated. Also, all the trees with a dbh >15 cm (i.e., adult trees) and with a dbh < 15 cm (i.e., young trees) were counted. The aboveground cover (i.e., shrubs, seedlings, herbs,

bare soil, adult and young trees) was always estimated within a 5-m radio around the trunk of each Holm oak and was used to complete their characterization. The aboveground cover was always estimated by consensus among four different observers to maintain the consistency of the data.

2.3. Soil sampling

Soil samples were collected from the three subplots established at each of the 13 study sites (cf. 2.2. *Experimental design and trees characterization*). Specifically, below each of the 9 Holm oaks selected within each subplot, 3 different soil samples were extracted around each tree to account for spatial heterogeneity. The 3 soil samples were extracted within a radius of 50 cm from the trunks of the 351 Holm oaks. This was done randomly as maintaining the exact same cardinal directions for all soil samples and Holm oaks was not always possible due to logistic issues (i.e., terrain characteristics such as big stones, big roots, etc.). In order to extract the soil samples, a metallic cylinder (5 cm diameter) was used. All samples were extracted from the first 10 cm of soil after leaf litter removal.

After sampling, 3 composite soil samples were available for each of the 3 subplots of all sites. To do so, for each subplot, all the soil samples collected below the 3 healthy Holm oaks were mixed in one bag, all the soil samples collected below the 3 affected Holm oaks were mixed in a second bag, and all the soil samples collected below the 3 dead Holm oaks were mixed in a third bag. Accordingly, a total of 9 composite soil samples were obtained for each of the study sites, and thus a total of 117 soil samples were available for the whole study.

Once collected, soil samples were immediately stored in a portable fridge where a 4 °C temperature was maintained until arrival to the laboratory. The composite soil samples were then homogenized and an aliquot of approx. 15 g from each of them was separated and frozen in order to preserve the natural structure of the microbial communities for subsequent soil microbial diversity analyses. Finally, the remaining soil samples were dried at room temperature, sieved using a 2 mm mesh size, and stored in a dry dark place until further analyses.

2.4. Soil biogeochemical variables

The pH of the 117 composite soil samples was measured by the saturated soil paste method (Kalra, 1995). Then, their total carbon (C) and nitrogen (N) were estimated using an elemental analyzer (Thermo Flash 2000, Thermo Fisher Scientific, Waltham, MA, USA). Soil organic carbon (SOC) content was estimated as the difference between the total C and the inorganic C in calcium carbonate ($CaCO_3$; Demolon and Leroux, 1952; Allison and Moodie, 1965). Additionally, available phosphorus (Av P) was estimated using the method described by Burriel and Hernando (1950) and an inductively coupled plasma optical emission spectrometer (PerkinElmer 4300 DV, PerkinElmer Inc., Wellesley, MA, USA). Specifically, this method uses an extracting solution composed of $CaCO_3$, $MgCO_3$, H_2SO_4 and acetic acid, with a pH between 3.2 and 3.3. Total phosphorous (Total P) was estimated by extraction with a mixture of strong acids (nitric + perchloric acid and heat on a hot plate following a method described in Allen, 1989; Isaac and Kerber, 1971 and an inductively coupled plasma optical emission spectrometer (PerkinElmer 4300 DV, PerkinElmer Inc., Wellesley, MA, USA). The cation concentration (Ca^{2+}, Mg^{+}, K^{+}, Na^{+}) of the composite soil samples were determined using an inductively coupled plasma optical emission spectrometer (PerkinElmer 4300 DV, PerkinElmer Inc., Wellesley, MA, USA) and an ammonium acetate extraction solution (pH = 7; M.A.P.A. 1986). To determine the amount of NO_3^- - N and ammonium (NH_4^+ - N) we used the Kjeldahl method (Kjeldahl, 1883) with a continuous flow analyzer (Skalar San++, Skalar Analytical B.V., Breda, The Netherlands). Finally, all soil biogeochemical variables were expressed per area (m^2) and 10 cm depth using the bulk density which was determined for each soil sample from the volume of the metallic cylinder that we used to extract the soil samples (McKenzie et al., 2004). For each composite soil sample, the amount found for a given soil variable (e.g., nutrients) was calculated in 10 cm of depth and 1 square meter (kg SOC m^{-2}, kg Total N m^{-2}, g Av P m^{-2}, g Total P m^{-2}, g Ca^{2+} m^{-2}, g Na^{+} m^{-2}, g Mg^{+} m^{-2}, mg NH_4^+-N m^{-2}, mg NO_3^-N m^{-2}).

2.5. Microbial C and N mineralization

From all 117 composite soil samples, the microbial C mineralization was measured as soil heterotrophic CO_2 production (i.e., respiration; R_H). For this, 40 g of dry soil were placed in a glass jar with a volume of 150 mL and rehydrated to reach 40% of the water holding capacity (WHC), following Lucas-Borja et al. (2016). To avoid the Birch effect (Birch, 1958), rehydrated soils were then incubated during 48 h maintaining constant the 40% WHC. Specifically, soil samples were subjected to a temperature response curve ranging from 5 to 35 °C, which roughly simulated a range of temperatures that soils could experience under Mediterranean climate. R_H was measured at each increase of 10 °C (i.e., waiting between measurements until the desired temperature was reached within the soil) over 60 s, using a portable soil gas exchange system (EGM-4, PP systems, MA, USA). The final R_H values represent an average of the four R_H values measured for each 10 °C temperature increase (i.e., 5 °C, 15 °C, 25 °C, and 35 °C). Besides, as a measurement of soil organic matter (SOM) turnover, we also calculated the R_H per unit of organic C, hereinafter referred to as "C turnover" (Curiel Yuste et al., 2007).

The net N mineralization (R_{min}) was also measured as the change over time in the concentration of soil mineral N (defined as the sum of NO_3^- - N and NH_4^+ - N) (Piccolo et al., 1994). Specifically, 40 g of dry soil (i.e., the same quantity we used for R_H estimations; see above) were incubated following a temperature response curve that ranged from 5 to 35 °C and from 35 to 5 °C during 15 days. Measurements were performed every 10 °C in cycles of 6 h. R_{min} was calculated as the differences in mineral N between day 15 and day 0 of the soil incubation period. Additionally, net ammonification (R_{amm}) and R_{nit} were calculated as the difference in ion ammonia and nitrate, respectively during the same incubation period (Piccolo et al., 1994). Rates of soil microbial C and N mineralization were normalized to area (m^2) and 10 cm depth (g CO_2 h^{-1} m^{-2}, mg NH_4^+-N day^{-1} m^{-2}, mg NO_3^-N day^{-1} m^{-2}, respectively), following the same procedure described before (cf. 2.4. *Soil biogeochemical variables*).

2.6. Soil microbial biomass

Soil microbial biomass was measured using a modified substrate-induced respiration (SIR) method (Anderson and Domsch, 1978) which estimates the living soil microbial biomass by measuring the maximum respiratory response of the soil samples after an excess of glucose is added. To do so, a subsample of 10 g of dry soil was placed in a glass jar and rehydrated to reach 40% of the water holding capacity (WHC). We then added 0.5 g glucose kg^{-1} of dried soil and incubated it for 2 h (i.e., the necessary time to have an initial maximum respiratory response before any increase in microbial biomass) at 30 °C. After the incubation, CO_2 emissions were measured over 60s using a portable soil gas exchange system (EGM-4, PP systems, MA, USA). These measurements were performed for each of the 117 composite soil samples.

2.7. DNA extraction, 16S and ITS amplicon sequencing

Soil DNA was extracted from the frozen soil aliquot that was separated immediately after sampling (cf. 2.3. *Soil sampling*). This was done using the PowerSoil DNA Isolation Kit (MoBio, CA, USA), following the manufacturer's recommendations. Once extracted, soil DNA was quantified using Qubit 3.0 (Invitrogen, CA, USA). To check its quality, an electrophoresis was carried out in a 0.8% (w/v) agarose gel stained with ethidium bromide. After that, soil DNA samples were sent to the Research Technology Support Facility at the Michigan State University where the construction of the amplicon libraries, according to the dual indexing strategy, was carried out (Kozich et al., 2013). Specifically, for bacteria, the V4–V5 regions of the 16S rRNA gene were amplified using the A515F and Y/926R primers described by Parada et al. (2016), while for fungi the ITS1 region was targeted using the ITS1FI2 and ITS2 primers (Schmidt et al., 2013). Each primer was then joined to their Illumina adaptor (Fluidigm CS1/CS2 oligos) and barcodes, allowing for the multiplexing of the samples. After the secondary PCR, each set of libraries was normalized using the Invitrogen SequalPrep DNA Normalization plates (ThermoFisher Scientific, Waltham, MA, USA) and the normalized DNA products were pooled. Once the pooled DNA was quantified and quality checked, each pool was loaded on an Illumina MiSeq v2 flow cell and sequenced with a PE250 strategy using a v2 500 cycle reagent kit. Finally, the base calling was made using Illumina Real Time Analysis (RTA) v1.18.54 and the output of RTA was then demultiplexed and converted to the FastQ format with Illumina Bcl2fastq v2.18.0.

2.8. Bioinformatic analyses of sequenced data

The FastQ files (cf. 2.7. *DNA extraction, 16S and ITS amplicon sequencing*) were pre-processed using the software FastQC (Andrews, 2010). This was done by taking into account the quality of the sequences and by removing Illumina adapters if present. After this first step, the reads were assembled using the pandaseq tool (Bartram et al., 2011) and setting the overlapping parameters by establishing a 0.9 threshold quality value for alignment and removing the primers. Once the reads were overlapped, the sequences were processed with Qiime 1.9.1 (Caporaso et al., 2010), which identifies and removes chimeras through USEARCH 6.1 by using the RDP gold database for bacteria and the UNITE chimera database for fungi. The resulting sequences were clustered into operational taxonomic units (OTUs) with an open-reference OTU picking process (pick_open_reference_otus from Qiime 1.9.1) at a 97% sequence identity to taxonomically assign the representative sequences for each OTU. For this, the RDP classifier database (i.e., with a threshold of 0.8) was used (Cole et al., 2014) as a reference. The process of clustering the fungal ITS sequences was similar to that used for bacteria but, in this case, the taxonomic identification of representative OTUs was made using the UNITE database as a reference. Finally, the resulting biom file was further used to carry out our analyses in R v. 3.5.1 (R Core Team, 2016) using the phyloseq v. 1.24.2 (McMurdie and Holmes, 2013) and vegan v. 2.5–4 (Oksanen et al., 2019) packages.

Overall, the functional groups directly associated with key paths of soil N cycling were targeted. Specifically, from the whole prokaryote and fungal communities, the following functional groups were targeted: ECM, which are specialized in improving the capacity of plants to uptake the soil mineral N; and nitrifiers, responsible for the transformation of the NH_4^+ - N into NO_3^- - N (i.e., R_{nit}). For this, FUNGuild (Nguyen et al., 2016), a tool that compares the taxonomic identification of the fungal community with a known database and assigns fungal guilds to all obtained fungal sequences, was used. Specifically, all fungal sequences assigned to the ECM guild were extracted. Several orders of the archaea [*Nitrososphaerales* (Kerou et al., 2018)] and bacteria [*Nitrosomonadales* (Wang and Chen, 2018), and *Nitrospirales* (Spieck and Bock, 2015)] kingdoms, involved in the process of nitrification, were also selected. A functional group that integrated them all was then created and referred to as nitrifiers hereinafter. Finally, the relative abundance of the ECM and nitrifiers was calculated for the 117 composite soil samples.

2.9. Statistical analyses

All variables were first checked for normality and log (e.g., SOC, total N, total P, NO_3^- - N, Ca^{2+}, microbial biomass, R_{nit}, R_H, C turnover) or square root (e.g., ECM, nitrifiers) transformed when the normality assumption was not met.

Differences in tree-related variables (i.e., see Table S1 for their complete list), aboveground cover (i.e., see Table S1 for their complete list), abiotic factors and percentage of crown coverage per ha (i.e., MAT, MAP, pH, and % Cc; see Table S3), and soil biogeochemical variables (i.e., see Table S4 for their complete list) between the different land-use types (i.e., FR, DH, and OW) were tested by performing one-way ANOVA analyses followed by a Tukey's Honest Significant Difference (HSD) post hoc test. Crown defoliation (i.e., healthy, affected, and dead Holm oaks) comparisons between different land-use types were also tested using one-way ANOVA analyses followed by a Tukey's Honest Significant Difference (HSD) post hoc test.

The effects of abiotic factors (i.e., MAT, MAP, and pH), land-use type (i.e., FR, DH, and OW), and crown defoliation (i.e., healthy, affected, and dead Holm oaks), as well as their interactions (i.e., the fixed part of the model) on all soil biogeochemical variables (i.e., see Table 2 for their complete list) and on all soil functional variables (i.e., see Table 3 for their complete list) were evaluated by running separate Linear Mixed-Effects models (LMEs) for each of them (Pinheiro et al., 2017). To run all these LMEs, a Boolean variable called "livestock grazing", which indicated the presence or absence of livestock at our study sites, was created. This was done to control for possible effects caused by grazing animals since the DH land-use type is usually used for livestock, while the FR and OW land-use types are not or not anymore (Pulido et al., 2010). This Boolean variable was introduced in the LMEs as nested within study sites and with a random effect. To control for data duplicity, the co-variance and multicollinearity of the fixed factors was first checked using the Variance Inflation Factor (VIF). All variables that had VIF values higher than 2 (Zuur et al., 2010) were eliminated from further analyses. Finally, the models that showed the lowest AIC (Akaike Information Criterion) values in each case were selected as being the best suited ones.

In order to see how the different soil biogeochemical and functional variables may be grouped into two linear axes that would explain the maximum amount of variance, a Principal Component Analysis (PCA) was performed (Fig. 2). For this, the effects of the abiotic factors (i.e., MAT, MAP, and pH) and land-use type (i.e., FR, DH, and OW) on soil biogeochemical and functional variables were first removed through the LMEs explained within the previous paragraph. Then, the residuals of the LMEs were used to run PCA by accounting for crown defoliation (i.e., healthy, affected, and dead Holm oaks). The results of the LMEs were further used to build and run a Structural Equation Model (SEM). For this, the "psem" function available from the piecewiseSEM package (Lefcheck, 2016), which allowed to introduce random effects (i.e., similar to the structure used for LMEs), was used. Specifically, the following explicative variables were introduced into SEM: abiotic factors (i.e., MAT, MAP, and pH) and crown defoliation (i.e., healthy, affected, and dead Holm oaks). The purpose was to search for all potential causal-effect relationships between explicative variables and all measured soil variables: biogeochemical, cycling, microbial C and N mineralization, and functional groups (ECM and nitrifiers). To test the good-

Table 2
Results of Linear Mixed-Effects models (LMEs): effects of abiotic factors (i.e., MAT, MAP, and pH), land-use type, and crown defoliation (i.e., healthy, affected, and dead Holm oaks), as well as their interactions (i.e., the fixed part of the model) on all soil biogeochemical variables. *P* – values marked in bold indicate significant or marginally significant relationships.

Response variables	Explanatory variables	Estimate	SE	df	t-value	*P*-value
SOC *	MAP	0.001	<0.001	101	1.978	**0.05**
	Crown defoliation	0.004	0.002	101	2.089	**0.04**
	MAP x Crown defoliation	−0.001	<0.001	101	−1.704	0.09
Total N *	Land-use type	−0.011	0.003	11	−3.119	**0.01**
	Crown defoliation	<0.001	<0.001	103	1.483	0.14
Total P *	MAT	0.244	0.093	10	2.631	**0.025**
	Land-use type	−0.009	0.005	10	−1.683	0.123
	Crown defoliation	0.001	<0.001	94	2.809	**0.006**
NH_4^+ - N	MAT	−86.006	39.269	11	−2.190	**0.05**
	MAP	−1.472	0.667	96	−2.206	**0.03**
	Crown defoliation	−6.712	3.434	96	−1.957	**0.05**
	MAT x MAP	0.128	0.05	96	2.511	**0.01**
	MAT x Crown defoliation	0.517	0.262	96	1.975	**0.05**
	MAP x Crown defoliation	0.01	0.005	96	2.181	**0.03**
	MAT x MAP x Crown defoliation	−0.001	<0.001	96	−2.224	**0.03**
NO_3^- - N *	MAT	0.098	0.117	11	0.840	0.42
	MAP	−0.002	0.001	102	−1.571	0.12
	Crown defoliation	0.005	0.001	102	3.790	<**0.001**
Av P	Crown defoliation	<0.001	<0.001	101	2.387	**0.02**
Ca^{2+} *	pH	0.467	0.043	100	10.951	<**0.001**
Na^+	Crown defoliation	−0.001	<0.001	102	−1.983	**0.05**
Mg^+	Crown defoliation	−0.014	0.005	103	−2.832	**0.0056**

Where, SE = standard error; MAP = mean annual precipitation; MAT = mean annual temperature; SOC = soil organic carbon; Total N = total nitrogen; Total P = total phosphorus; NH_4^+ - N = soil ammonium content; NO_3^- - N = soil nitrate content; Av P = available phosphorus; Ca^{2+} = calcium; Na^+ = sodium; Mg^+ = magnesium. Variables marked with * have been log transformed.

ness of fit of the SEM, the Fisher's C statistic, which follows a chi-squared distribution and tests if the model fits the data ($P > 0.05$) or not ($P < 0.05$), was calculated. The final SEM selection was based on the AIC coefficient (Lefcheck, 2016).

All statistical analyses were carried out in R v. 3.5.1 (R Core Team, 2016). Relationships for all our statistical analyses were considered significant at $P < 0.05$.

Table 3
Results of Linear Mixed-Effects models (LMEs): effects of abiotic factors (i.e., MAT, MAP, and pH), land-use type, and crown defoliation (i.e., healthy, affected, and dead Holm oaks), as well as their interactions (i.e., the fixed part of the model) on all soil functional variables. *P* – values marked in bold indicate significant or marginally significant relationships.

Response variables	Explanatory variables	Estimate	SE	df	t-value	*P*-value
Microbial biomass *	pH	0.263	0.057	103	4.61	<**0.001**
nitrifiers **	MAP	−0.001	0.000	94	−2.160	**0.03**
	Crown defoliation	0.001	0.001	94	3.752	<**0.001**
ECM **	Crown defoliation	−0.013	0.003	99	−4.280	<**0.001**
R_{amm}	MAP	0.027	0.012	100	2.312	**0.02**
	Crown defoliation	−0.041	0.011	100	−3.615	<**0.001**
R_{nit} *	pH	0.264	0.127	97	2.081	**0.04**
	Crown defoliation	0.005	0.001	97	3.246	**0.002**
R_H *	pH	0.537	0.068	101	7.900	<**0.001**
	Crown defoliation	−0.001	<0.001	101	−2.012	**0.05**
C turnover *	pH	0.510	0.073	99	7.01	<**0.001**
	Crown defoliation	−0.001	0.000	99	−2.368	**0.02**

Where, SE = standard error; MAP = mean annual precipitation; ECM = ectomycorrhizal fungi; R_{amm} = net ammonification; R_{nit} = net nitrification; R_H = heterotrophic respiration; C turnover = R_H per unit of SOC. Variables marked with * have been log transformed, while variables marked with ** have been square root transformed.

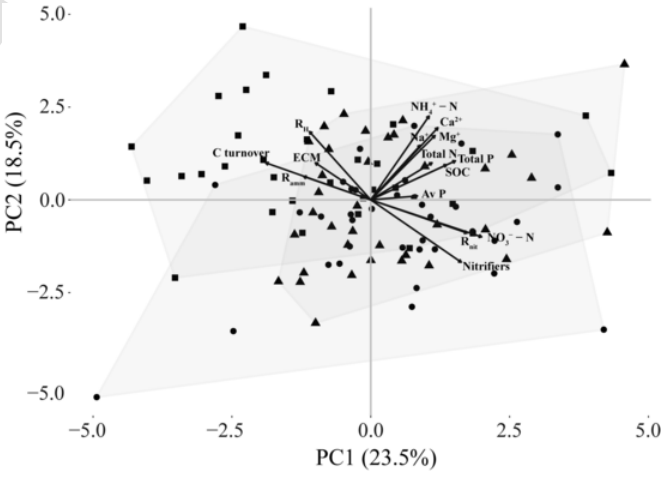

Fig. 2. Principal Component Analysis (PCA) results showing how soil biogeochemical and functional variables may be grouped into two linear axes as a function of crown defoliation. Square symbols represent healthy Holm oaks, triangle ones represent affected Holm oaks, and circle ones represent dead Holm oaks. *Where*, C turnover = R_H per unit of SOC; R_H = heterotrophic respiration; ECM = ectomycorrhizal fungi; R_{amm} = net ammonification; NH_4^+ - N = soil ammonium content; Ca^{2+} = calcium; Na^+ = sodium; Mg^+ = magnesium; Total N = total nitrogen; Total P = total phosphorus; SOC = soil organic carbon; Av P = available phosphorus; R_{nit} = net nitrification; NO_3^- - N = soil nitrate content.

3. Results

3.1. Aboveground cover structure as a function of land-use type and crown defoliation

The aboveground cover, estimated around each of our 351 Holm oaks, varied across the different land-use types (i.e., FR, DH, and OW) and the different crown defoliation levels (i.e., healthy, affected, and dead trees) (Tables S1 and S2). Specifically, the DH land-use type had a significantly higher herbaceous cover than FR and OW (Table S1). The DH land-use type also had trees with larger canopies and dbh than the FR and OW land-use types (Table S1). Trees from OW were shortest (Table S1). Vegetation area index (VAI) values and the total number of trees (i.e., adult and young), around the selected Holm oaks, were significantly lower in DH compared to FR and OW (Table S1). A significant decrease in VAI with tree crown cover and death was also observed for OW and DH, but not for FR (Table S2). Also, the percentage of bare soil in DH increased significantly with tree crown defoliation and death (Table S2). ANOVA and subsequent post hoc analyses further showed that DH are on average warmer (i.e., higher MAT), wetter (i.e., higher MAP), and have a more acidic soil (i.e., lower pH) than FR and OW (Table S3).

3.2. Variability in soil variables associated with differences in land-use type, abiotic variables, and crown defoliation

LMEs results showed that abiotic factors (i.e., MAT, MAP, and pH) and crown defoliation (i.e., healthy, affected, and dead) were the main explanatory variables that showed additive and interactive effects on the analyzed soil variables (Tables 2 and 3). Still, only total N showed a negative relation with land-use type, the land-use types with lower crown coverage having more N (DH than OW and FR) (Table 2), while the remaining soil variables showed higher sensitivity to MAP variability rather than to MAT variability (Tables 2 and 3). Specifically, MAP affected positively SOC (Table 2) and R_{amm} (Table 3), and negatively the pools of mineral N (Table 2) and the nitrifiers (Table 3). On the other hand, soil pH affected the capacity of soils to oxidize NH_4^+ - N by controlling the amount of soil available NH_4^+ - N (i.e., a decrease in pH resulted in the liberation of NH_4^+ - N, see Table 3) further affecting R_{nit} rates. Furthermore, soil pH was positively correlated with soil microbial biomass and R_H (Table 3).

Overall, crown defoliation was the factor that was best correlated with soil pools, microbial C and N mineralization, and relative abundances of functional groups (Tables 2 and 3; Fig. 2 and 3). For instance, SOC was positively correlated with both MAP and crown defoliation (Table 2). Moreover, crown defoliation and subsequent death was related to lower rates of soil C turnover (R_H per unit of SOC) (Table 3), resulting also in higher rates of mineralization of N (hence crown defoliation affected negatively both R_H and R_{amm}; Figs. 2 and 3). Crown defoliation was also strongly associated with the accumulation of Av P and total P but also with net losses of essential ions such as Mg^{2+} and Na^+ (Table 2). Overall, we observed an especially strong influence of crown defoliation over pools, soil metabolic pathways and functional guilds strongly associated with the N cycle (Table 3, Fig. 3). Crown defoliation was associated with large changes in the ECM (decrease) and nitrifiers (increase) communities resulting in higher rates of R_{nit} (Fig. 3) and high concentrations of NO_3^- - N and low concentrations of NH_4^+ - N under dead trees (Table 2). These alterations further lead to high concentrations of the most mobile forms of N (NO_3^- - N) and P (Av P) related to the observed relatively high relative abundance of nitrifiers and low relative abundance of ECM (Table 3; Figs. 2 and 3) under defoliated crowns. Moreover, our results show also how nitrifiers play an important role by being associated with low concentrations of NH_4^+ - N and high rates of R_{nit} (Fig. 3).

4. Discussion

Our study provides evidence that there are strong drought-induced tree mortality effects on soil biogeochemical cycling, rates of microbial C and N mineralization, and relative abundances of key functional groups (ECM and nitrifiers). This phenomenon may, in many cases, obscure and/or exacerbate the direct effects of climate over soils, which in this study was represented by a wide climatic gradient across the Spanish Iberian Peninsula. These results are of great importance given

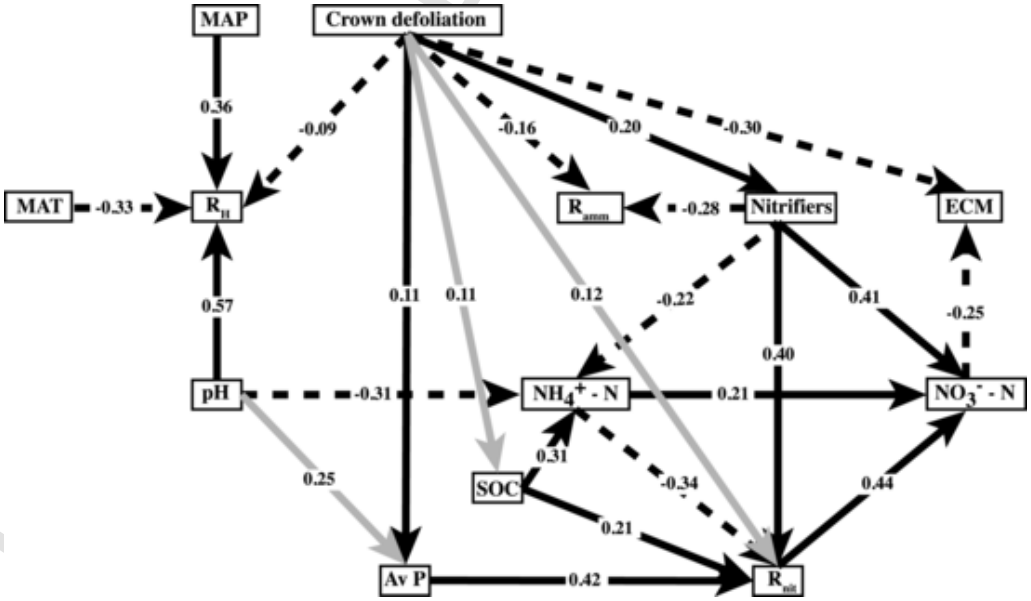

Fig. 3. Structural Equation Model (SEM) results. The path diagram represents hypothesized causal relationships between abiotic factors (i.e., MAT, MAP, and pH), crown defoliation (i.e., healthy, affected, and dead Holm oaks), and soil biogeochemical variables, microbial C and N mineralization, and functional groups. Causal relationships are indicated by arrows as follows: positive and negative effects are indicated by solid and dashed lines respectively, and numbers indicate the standardized estimated regressions weights (SRW). Black arrows represent significant relationships, while grey arrows represent marginally significant relationships. *Where*, MAT = mean annual temperature; MAP = mean annual precipitation; R_H = heterotrophic respiration; Av P = available phosphorus; SOC = soil organic carbon; R_{amm} = net ammonification; NH_4^+ - N = soil ammonium content; R_{nit} = net nitrification; NO_3^- - N = soil nitrate content; ECM = ectomycorrhizal fungi.

the increasingly frequent and severe drought events which are causing drought-related tree decline and mortality rates all over the world (Allen et al., 2010, 2015; Hartmann et al., 2018). Our results indicate that drought-induced tree mortality could potentially aggravate the expected negative effects of hotter and drier climates associated with climate change on soil biogeochemical cycling, microbial C and N mineralization, and key functional groups. However, accounting for this phenomenon in predictions requires to take into consideration some of the complex interactions and the exchanges of energy and matter occurring between plants and soil, interactions that soil models, e.g., RothC (Jenkinson and Rayner, 2006), CENTURY (Parton et al., 1987; Paustian et al., 1992) or Yasso (Tuomi et al., 2011; Liski et al., 2005) are currently not taking into account. This reductionist approach could be a potential reason for the difficulties that we have to correctly simulate the impacts of climate extremes on soil biogeochemical cycling, forest stability and subsequent climate feedbacks (Reichstein et al., 2013; Bahn et al., 2014).

As precipitation (i.e., MAP) decreased with latitude, it limited the accumulation of soil C, but also affected key soil functions involved in N and C cycling, such as R_{amm} and R_H. This is not surprising, since it is well known that microbial activity is very sensitive to changes in water availability (e.g., Sardans and Peñuelas, 2005, Curiel Yuste et al., 2007; Curiel Yuste et al., 2011). Indeed, our precipitation gradient shows how water limits the capacity of soil microbiota to decompose SOM, hence altering R_H (Curiel Yuste et al., 2007; Moyano et al., 2012; Sardans and Peñuelas, 2013) as well as other functions related to N mineralization (Chen et al., 2011; Larsen et al., 2011; Xu et al., 2016).

Holm oak crown defoliation and subsequent death triggered a cascade of causal-effect processes that exacerbated the potential and well documented effects of drought over soil biogeochemical variables, microbial C and N mineralization, and functional groups (ECM and nitrifiers). These findings point to drought-induced tree decline and mortality as a highly important factor that should be taken into account in order to better understand how ongoing changes at local scales could potentially affect soil C and nutrient cycling at regional and global scales (Sardans and Peñuelas, 2013; Gómez-Aparicio et al., 2017; Curiel Yuste et al., 2019). For instance, crown defoliation was, together with precipitation, the only variable that explained most of the observed changes in SOC sequestration. Accumulation of senescent leaves and fine roots (Curiel Yuste et al., 2019) together with the observed decrease in C turnover rates following the reduction in labile C inputs that stimulate R_H (e.g., root exudates; see Kuzyakov, 2002; Blagodatskaya and Kuzyakov, 2008) could explain this increase in SOC associated with crown defoliation. Crown defoliation was also related to further stoichiometric imbalances, resulting in alterations of soil nutrient concentrations (e.g., losses of essential oligonutrients such as Mg^{2+} and Na^{+}) and the transformation of other nutrients into mobile forms (NO_3^- - N and Av P) that may be accumulated in the soil instead of being taken up by plants. These stoichiometric imbalances could further hinder the recovery (e.g., Holm oak regeneration) of these highly human-transformed ecosystems because, e.g., Mg^{2+} is an essential constituent of the rubisco enzyme and unused mobile forms of N and P could be easily leached out of the system (e.g., Koskinen et al., 2011). Hence, nutrient losses and soil stoichiometry imbalances associated with tree mortality could hasten the conversion of these woodlands into shrublands or grasslands (Fensham et al., 2009; Anderegg et al., 2012) further affecting the C and nutrient source/sink dynamics (Adams et al., 2010; Hicke et al., 2012). Particularly, the observed lack of recruitment (% of non-herbaceous vegetation) and the decrease of the vegetation area index (VAI) after tree mortality, observed under more intensively managed sites (OW and DH), support this idea and suggest that the capacity of these ecosystems to recover after tree mortality events could be compromised.

Tree mortality effects were especially intense over the metabolic paths involving soil N cycling, obscuring in many cases the well-known sensitivity to drought of key N processes such as R_{nit} (Chen et al., 2011). This is consistent with previous results showing how severely the N cycle could be affected by the declining tree health and subsequent mortality (Edburg et al., 2012; Avila et al., 2016; Rodríguez et al., 2017). The results of the SEM showed imbalances in the production/consumption of mineral forms of N (NH_4^+ - N and NO_3^- - N) mediated to a large extent by the change in the relative abundance of key microbial functional groups involved in N cycling. Tree mortality resulted in an accumulation of mobile forms of N (NO_3^- - N) due to the stimulation of the transformation of NH_4^+ - N into NO_3^- - N (R_{nit}). This increase in the soil concentration of the most mobile form of N (i.e., NO_3^- - N), associated with crown defoliation and tree mortality, was positively associated with the proliferation of nitrifiers and the decrease in ECM, responsible for the uptake of soil N for plant consumption (Koide et al., 2014). The accumulation of the most mobile form of N (i.e., NO_3^- - N) under defoliated crowns, therefore, resulted not only from the increase in the R_{nit} but also from the decrease in its consumption by vegetation, evidenced by the disruption of the symbiotic plant-fungus relationship (ECM) as tree health declined. While this increase in the production and subsequent accumulation of NO_3^- - N following tree mortality has not been identified before, it was, according to our SEM, further facilitated by the parallel increase in Av P, which generally becomes a limiting nutrient when N is not limiting (He and Dijkstra, 2015; Deng et al., 2017). Hence, net increases in mobile forms of essential nutrients during tree decline and mortality could easily result in net losses of these essential nutrients from the system. For instance, the accumulation of mobile forms of N (i.e., NO_3^- - N), associated with tree mortality, may stimulate denitrification processes and lead to emissions of N oxides (e.g., N_2O) to the atmosphere (Li et al., 2016). NO_3^- - N accumulation, together with mobile forms of P (i.e., Av P), might also lead to losses of N and P through leaching to aquifers or other water sources, which could potentially alter water quality (e.g., eutrophication) as well as deteriorate soils, further accelerating the process of conversion into shrublands or grasslands (Stark and Richards, 2008).

5. Conclusions

An in-depth understanding of how drought-induced tree decline and mortality alters plant-soil relationships are needed in order to better understand climate-change effects on soil C and nutrient cycling. In fact, direct alterations resulting from the climatic changes towards hotter and drier climatic conditions that are already occurring in the Spanish Iberian Peninsula were obscured and/or exacerbated by the effect of tree crown defoliation and mortality. Holm oak crown defoliation and mortality trigger a cascade of causal-effect relationships leading to important changes in the relative abundance of key soil microbial functional groups such as nitrifiers and ECM that resulted in important transformations of some of the metabolic pathways controlling N and P cycling. There may be many consequences of accumulation of mobile forms of N (NO^{3-} - N) or P (Av P) associated with tree mortality: stimulation of denitrification which leads to emissions of N oxides (e.g., N_2O) to the atmosphere; leaching of these mobile forms of N and P to aquifers or other water sources, which could potentially alter water quality (e.g., eutrophication) as well as deteriorate soils; or accelerating the process of conversion into shrublands or grasslands. By integrating into models knowledge on the mechanisms that relate tree mortality to key metabolic pathways that control the cycling of C, N, and P and other essential oligonutrients (e.g., Mg^{2+}) our predictions of climate change effects on soil biogeochemical cycling might substantially improve.

Data availability

The datasets analyzed in this study are available in the NCBI Sequence Read Archive (SRA) repository (www.ncbi.nlm.nih.gov/sra) under the BioProject accession number PRJNA529407.

Declaration of competing interest

The authors declare that they have no known competing financial interests or personal relationships that could have appeared to influence the work reported in this paper.

Acknowledgements

This research was supported by the VERONICA (CGL2013-42271-P) and IBERYCA (CGL2017-84723-P) projects, both funded by the Spanish Government. D. García-Angulo was financed through a FPI fellowship (BES-2014-067971) from the Spanish Ministry of Science, Innovation and Universities, and O. Flores through a FPU fellowship (FPU14/05408) from the Spanish Ministry of Education, Culture and Sport. This research was also supported by the Basque Government through the BERC 2018–2021 program, and by the Spanish Ministry of Science, Innovation and Universities through the BC3 María de Maeztu excellence accreditation (MDM-2017-0714). This work was also financed by the NATIvE (PN-III-P1-1.1-PD-2016-0583) project through UEFISCDI (Romanian Ministry of Education and Research). We thank Nutrilab for their technical and analytical support, and Miguel Fernandez, David López Quiroga, Gerardo Moreno, Alejandro Solla, Andrea Orejarena, Sonia Novella, Ana Rincón, Barbara Carvalho, Matheus Lopes Souza, Octavio Cedenilla, Elisa Garzo, Alexandra Rodriguez, Jorge Durán and Mario Díaz for their priceless support during the field campaigns and the laboratory work.

Appendix A. Supplementary data

Supplementary data related to this article can be found at https://doi.org/10.1016/j.soilbio.2020.107921.

References

Adams, H D, Macalady, A K, Breshears, D D, Allen, C D, Stephenson, N L, Saleska, S R, Huxman, T E, McDowell, Ng, 2010. Climate-induced tree mortality: earth system consequences. Eos, Transactions American Geophysical Union 91, 153–154.

Allen, C D, Macalady, A K, Chenchouni, H, Bachelet, D, McDowell, N, Vennetier, M, Kitzberger, T, Rigling, A, Breshears, D D, Hogg, E H, Gonzalez, P, Fensham, R, Zhang, Z, Castro, J, Demidova, N, Lim, J-H, Allard, G, Running, S W, Semerci, A, Cobb, N, 2010. A global overview of drought and heat-induced tree mortality reveals emerging climate change risks for forests. Forest Ecology and Management 259, 660–684.

Allen, S E, 1989. Chemical Analysis of Ecological Materials, 2nd ed. Blackwell, Oxford.

Allen, C D, Breshears, D D, McDowell, N G, 2015. On underestimation of global vulnerability to tree mortality and forest die-off from hotter drought in the Anthropocene. Ecosphere 6, art129.

Allison, L E, Moodie, C D, 1965. Carbonate. In: Black, C A (Ed.), Methods of Soil Analysis. Part 2. Chemical and Microbiological Properties. American Society of Agronomy, Madison, Wi, pp. 1379–1396.

Anderegg, W R L, Kane, J M, Anderegg, L D L, 2012. Consequences of widespread tree mortality triggered by drought and temperature stress. Nature Climate Change 3, 30.

Anderson, J P E, Domsch, K H, 1978. A physiological method for the quantitative measurement of microbial biomass in soils. Soil Biology and Biochemistry 10, 215–221.

S. Andrews FastQC A quality control tool for high throughput sequence datahttp://www.bioinformatics.babraham.ac.uk/projects/fastqc/2010

M.A.P.A., 1986. Métodos oficiales de análisis. Tomo III. Plantas, productos orgánicos fertilizantes, suelos, agua, productos fitosanitarios y fertilizantes inorgánicos. Publicaciones del Ministerio de Agricultura, Pesca y Alimentación, Madrid.

IPCC, Field, C B, Barros, V R, Dokken, D J, K.J., 2014. Impacts, Adaptation, and Vulnerability. Part a: Global and Sectoral Aspects. Contribution of Working Group II to the Fifth Assessment Report of the Intergovernmental Panel on Climate Change. Cambridge University Press, United Kingdom and New York.

Avila, J M, Gallardo, A, Ibáñez, B, Gómez-Aparicio, L, Turnbull, M, 2016. *Quercus suber* dieback alters soil respiration and nutrient availability in Mediterranean forests. Journal of Ecology 104, 1441–1452.

Avila, J M, Gallardo, A, Gómez-Aparicio, L, 2019. Pathogen-induced tree mortality interacts with predicted climate change to alter soil respiration and nutrient availability in Mediterranean systems. Biogeochemistry 142, 53–71.

Bahn, M, Reichstein, M, Dukes, J S, Smith, M D, McDowell, N G, 2014. Climate–biosphere interactions in a more extreme world. New Phytologist 202, 356–359.

Barnard, R L, Osborne, C A, Firestone, M K, 2013. Responses of soil bacterial and fungal communities to extreme desiccation and rewetting. The ISME Journal 7, 2229–2241.

Bartram, A K, Lynch, M D J, Stearns, J C, Moreno-Hagelsieb, G, Neufeld, J D, 2011. Generation of multimillion-sequence 16S rRNA gene libraries from complex microbial communities by assembling paired-end Illumina reads. Applied and Environmental Microbiology 77, 3846–3852.

Birch, H F, 1958. The effect of soil drying on humus decomposition and nitrogen availability. Plant and Soil 10, 9–31.

Blagodatskaya, E, Kuzyakov, Y, 2008. Mechanisms of real and apparent priming effects and their dependence on soil microbial biomass and community structure: critical review. Biology and Fertility of Soils 45, 115–131.

Burriel, F, Hernando, V, 1950. El fósforo en los suelos españoles. V. Nuevo método para la determinar el fósforo asimilable en los suelos. Anales de Edafologia y Agrobiologia 9, 611–622.

Camarero, J J, Franquesa, M, Sangüesa-Barreda, G, 2015. Timing of Drought Triggers Distinct Growth Responses in Holm Oak: Implications to Predict Warming-Induced Forest Defoliation and Growth Decline. Forests 6, 1576–1597. doi:https://doi.org/10.3390/f6051576.

Camarero, J J, Sangüesa-Barreda, G, Vergarechea, M, 2016. Prior height, growth, and wood anatomy differently predispose to drought-induced dieback in two Mediterranean oak species. Annals of Forest Science 73, 341–351. doi:https://doi.org/10.1007/s13595-015-0523-4.

Caporaso, J G, Kuczynski, J, Stombaugh, J, Bittinger, K, Bushman, F D, Costello, E K, Fierer, N, Peña, A G, Goodrich, J K, Gordon, J I, Huttley, G A, Kelley, S T, Knights, D, Koenig, J E, Ley, R E, Lozupone, C A, McDonald, D, Muegge, B D, Pirrung, M, Reeder, J, Sevinsky, J R, Turnbaugh, P J, Walters, W A, Widmann, J, Yatsunenko, T, Zaneveld, J, Knight, R, 2010. QIIME allows analysis of high-throughput community sequencing data. Nature Methods 7, 335.

Casals, P, Gimeno, C, Carrara, A, Lopez-Sangil, L, Sanz, M, 2009. Soil CO_2 efflux and extractable organic carbon fractions under simulated precipitation events in a Mediterranean Dehesa. Soil Biology and Biochemistry 41, 1915–1922.

Chen, Y-T, Borken, W, Stange, C F, Matzner, E, 2011. Effects of decreasing water potential on gross ammonification and nitrification in an acid coniferous forest soil. Soil Biology and Biochemistry 43, 333–338.

Cole, J R, Wang, Q, Fish, J A, Chai, B, McGarrell, D M, Sun, Y, Brown, C T, Porras-Alfaro, A, Kuske, C R, Tiedje, J M, 2014. Ribosomal Database Project: data and tools for high throughput rRNA analysis. Nucleic Acids Research 42, D633–D642.

Corcobado, T, Cubera, E, Juárez, E, Moreno, G, Solla, A, 2014. Drought events determine performance of *Quercus ilex* seedlings and increase their susceptibility to *Phytophthora cinnamomi*. Agricultural and Forest Meteorology 192–193, 1–8.

Curiel Yuste, J, Baldocchi, D D, Gershenson, A, Goldstein, A, Misson, L, Wong, S, 2007. Microbial soil respiration and its dependency on carbon inputs, soil temperature and moisture. Global Change Biology 13, 2018–2035.

Curiel Yuste, J, Peñuelas, J, Estiarte, M, Garcia-Mas, J, Mattana, S, Ogaya, R, Pujol, M, Sardans, J, 2011. Drought-resistant fungi control soil organic matter decomposition and its response to temperature. Global Change Biology 17, 1475–1486.

Curiel Yuste, J, Barba, J, Fernández-González, A J, Fernández-López, M, Mattana, S, Martínez-Vilalta, J, Nolis, P, Lloret, F, 2012. Changes in soil bacterial community triggered by drought-induced gap succesion preceded changes in soil C stocks and quality. Ecology and Evolution 2, 3016–3031.

Curiel Yuste, J, Fernández-González, A J, Fernández-López, M, Ogaya, R, Peñuelas, J, Sardans, J, Lloret, F, 2014. Strong functional stability of soil microbial communities under semiarid Mediterranean conditions and subjected to long-term shifts in baseline precipitation. Soil Biology and Biochemistry 69, 223–233.

Curiel Yuste, J, Hereş, A-M, Ojeda, G, Paz, A, Pizano, C, García-Angulo, D, Lasso, E, 2017. Soil heterotrophic CO_2 emissions from tropical high-elevation ecosystems (Páramos) and their sensitivity to temperature and moisture fluctuations. Soil Biology and Biochemistry 110, 8–11.

Curiel Yuste, J, Flores-Rentería, D, García-Angulo, D, Hereş, A M, Bragă, C, Petritan, A M, Petritan, I C, 2019. Cascading effects associated with climate-change-induced conifer mortality in mountain temperate forests result in hot-spots of soil CO_2 emissions. Soil Biology and Biochemistry 133, 50–59.

de Sampaio e Paiva Camilo-Alves, C, da Clara, M I E, de Almeida Ribeiro, N M C, 2013. Decline of Mediterranean oak trees and its association with *Phytophthora cinnamomi*: a review. European Journal of Forest Research 132, 411–432.

Demolon, A, Leroux, D, 1952. Guide pour l'Étude expérimentale du Sol. Second edition. Soil Science 74, 405.

Deng, Q, Hui, D, Dennis, S, Reddy, K C, 2017. Responses of terrestrial ecosystem phosphorus cycling to nitrogen addition: a meta-analysis. Global Ecology and Biogeography 26, 713–728.

Dobbertin, M, 2006. Tree growth as indicator of tree vitality and of tree reaction to environmental stress: a review. European Journal of Forest Research 124, 319–333.

Edburg, S L, Hicke, J A, Brooks, P D, Pendall, E G, Ewers, B E, Norton, U, Gochis, D, Gutmann, E D, Meddens, A J, 2012. Cascading impacts of bark beetle-caused tree mortality on coupled biogeophysical and biogeochemical processes. Frontiers in Ecology and the Environment 10, 416–424.

Felicísimo, ÁM, Muñoz, J, Villalba, C J, Mateo, R G, 2011. Impactos, vulnerabilidad y adaptación al cambio climático de la biodiversidad española. 1. Flora y vegetación. Oficina Española de Cambio Climático, Ministerio de Medio Ambiente y Medio Rural y Marino, Madrid.

Fensham, R J, Fairfax, R J, Ward, D P, 2009. Drought-induced tree death in savanna. Global Change Biology 15, 380–387.

Flores-Rentería, D, Rincón, A, Morán-López, T, Hereş, A-M, Pérez-Izquierdo, L, Valladares, F, Curiel Yuste, J, 2018. Habitat fragmentation is linked to cascading effects on soil functioning and CO_2 emissions in Mediterranean holm-oak-forests. PeerJ 6, e5857.

Gómez-Aparicio, L, Domínguez-Begines, J, Kardol, P, Ávila, J M, Ibáñez, B, García, L V, 2017. Plant-soil feedbacks in declining forests: implications for species coexistence. Ecology 98, 1908–1921.

Hartmann, H, Moura, C F, Anderegg, W R L, Ruehr, N K, Salmon, Y, Allen, C D, Arndt, S K, Breshears, D D, Davi, H, Galbraith, D, Ruthrof, K X, Wunder, J, Adams, H D, Bloemen, J, Cailleret, M, Cobb, R, Gessler, A, Grams, T E E, Jansen, S, Kautz, M, Lloret, F, O'Brien, M, 2018. Research frontiers for improving our understanding of drought-induced tree and forest mortality. New Phytologist 218, 15–28.

He, M, Dijkstra, F A, 2015. Phosphorus addition enhances loss of nitrogen in a phosphorus-poor soil. Soil Biology and Biochemistry 82, 99–106.

Hereş, A-M, Kaye, M W, Granda, E, Benavides, R, Lázaro-Nogal, A, Rubio-Casal, A E, Valladares, F, Curiel Yuste, J, 2018. Tree vigour influences secondary growth but not responsiveness to climatic variability in Holm oak. Dendrochronologia 49, 68–76.

Herguido Sevillano, E, Lavado Contador, J F, Pulido, M, Schnabel, S, 2017. Spatial patterns of lost and remaining trees in the Iberian wooded rangelands. Applied Geography 87, 170–183.

Hicke, J A, Allen, C D, Desai, A R, Dietze, M C, Hall, R J, Hogg, E H, Kashian, D M, Moore, D, Raffa, K F, Sturrock, R N, Vogelmann, J, 2012. Effects of biotic disturbances on forest carbon cycling in the United States and Canada. Global Change Biology 18, 7–34.

Högberg, P, Nordgren, A, Buchmann, N, Taylor, A F S, Ekblad, A, Högberg, M N, Nyberg, G, Ottosson-Löfvenius, M, Read, D J, 2001. Large-scale forest girdling shows that current photosynthesis drives soil respiration. Nature 411, 789–792.

Isaac, R A, Kerber, J D, et al., 1971. Atomic Absorption and Flame Photometry: Techniques and Uses in Soil, Plant, and Water Analysis. Instrumental Methods for Analysis of Soils and Plant Tissue, L.M. Walsh ASA, CSSA, and SSSA Books.

Jenkinson, D S, Rayner, J H, 2006. The turnover of soil organic matter in some of the rothamsted classical experiments. Soil Science 171, S130–S137.

Kalra, Y P, 1995. Determination of pH of soils by different methods: collaborative study. Journal of AOAC International 78, 310–324.

Kerou, M, Alves, R J, Schleper, C, 2018. Nitrososphaerales. In: Whitman, W B, Rainey, F, Kämpfer, P, Trujillo, M, Chun, J, DeVos, P, Hedlund, B, Dedysh, S (Eds.), Bergey's Manual of Systematics of Archaea and Bacteria New York, NY.

Kjeldahl, J, 1883. Neue Methode zur Bestimmung des Stickstoffs in organischen Körpern. Zeitschrift für Analytische Chemie 22, 366–382.

Koide, R T, Fernandez, C, Malcolm, G, 2014. Determining place and process: functional traits of ectomycorrhizal fungi that affect both community structure and ecosystem function. New Phytologist 201, 433–439.

Koskinen, M, Sallantaus, T, Vasander, H, 2011. Post-restoration development of organic carbon and nutrient leaching from two ecohydrologically different peatland sites. Ecological Engineering 37, 1008–1016.

Kozich, J J, Westcott, S L, Baxter, N T, Highlander, S K, Schloss, P D, 2013. Development of a dual-index sequencing strategy and curation pipeline for analyzing amplicon sequence data on the MiSeq Illumina sequencing platform. Applied and Environmental Microbiology 79, 5112–5120.

Kuzyakov, Y, 2002. Review: factors affecting rhizosphere priming effects. Journal of Plant Nutrition and Soil Science 165, 382–396.

Larsen, K S, Andresen, L C, Beier, C, Jonasson, S, Albert, K R, Ambus, P, Arndal, M F, Carter, M S, Christensen, S, Holmstrup, M, Ibrom, A, Kongstad, J, Van Der Linden, L, Maraldo, K, Michelsen, A, Mikkelsen, T N, Pilegaard, K, Priemé, A, Ro-Poulsen, H, Schmidt, I K, Selsted, M B, Stevnbak, K, 2011. Reduced N cycling in response to elevated CO_2, warming, and drought in a Danish heathland: synthesizing results of the CLIMAITE project after two years of treatments. Global Change Biology 17, 1884–1899.

Lefcheck, J S, 2016. piecewiseSEM: piecewise structural equation modelling in r for ecology, evolution, and systematics. Methods in Ecology and Evolution 7, 573–579.

Li, X, Sørensen, P, Olesen, J E, Petersen, S O, 2016. Evidence for denitrification as main source of N2O emission from residue-amended soil. Soil Biology and Biochemistry 92, 153–160.

Liski, J, Palosuo, T, Peltoniemi, M, Sievänen, R, 2005. Carbon and decomposition model Yasso for forest soils. Ecological Modelling 189, 168–182.

Lloret, F, Siscart, D, Dalmases, C, 2004. Canopy recovery after drought dieback in holm-oak Mediterranean forests of Catalonia (NE Spain). Global Change Biology 10, 2092–2099.

Lloret, F, Mattana, S, Curiel Yuste, J, 2015. Climate-induced die-off affects plant–soil–microbe ecological relationship and functioning. FEMS Microbiology Ecology 91, 1–12.

Lucas-Borja, M E, Hedo, J, Cerdá, A, Candel-Pérez, D, Viñegla, B, 2016. Unravelling the importance of forest age stand and forest structure driving microbiological soil properties, enzymatic activities and soil nutrients content in Mediterranean Spanish black pine (*Pinus nigra Ar. ssp. salzmannii*) Forest. The Science of the Total Environment 562, 145–154.

Ma, S, Baldocchi, D D, Hatala, J A, Detto, M, Curiel Yuste, J, 2012. Are rain-induced ecosystem respiration pulses enhanced by legacies of antecedent photodegradation in semi-arid environments? Agricultural and Forest Meteorology 154–155, 203–213.

MAGRAMA, 2007. Tercer Inventario Forestal Nacional (IFN3). Ministerio de Agricultura, Alimentación y Medio Ambiente, Spain.

Mariotti, A, Pan, Y, Zeng, N, Alessandri, A, 2015. Long-term climate change in the Mediterranean region in the midst of decadal variability. Climate Dynamics 44, 1437–1456.

McDowell, N G, Michaletz, S T, Bennett, K E, Solander, K C, Xu, C, Maxwell, R M, Middleton, R S, 2018. Predicting chronic climate-driven disturbances and their mitigation. Trends in Ecology & Evolution 33, 15–27.

McKenzie, N J, Jacquier, D J, Isbell, R F, Brown, K L, 2004. Australian Soils and Landscapes an Illustrated Compendium. CSIRO Publishing, Collingwood, Victoria.

McMurdie, P J, Holmes, S, 2013. Phyloseq: an R package for reproducible interactive analysis and graphics of microbiome census data. PloS One 8, e61217.

Medina, N G, Lara, F, Mazimpaka, V, Albertos, B, Alonso, I, Hortal, J, 2015. Epiphytic bryophytes of *quercus* forests in central and north inland Iberian Peninsula. Frontiers of Biogeography 7, 21–28.

Moreno-Jiménez, E, Plaza, C, Saiz, H, Manzano, R, Flagmeier, M, Maestre, F T, 2019. Aridity and reduced soil micronutrient availability in global drylands. Nature Sustainability 2, 371–377.

Moyano, F E, Vasilyeva, N, Bouckaert, L, Cook, F, Craine, J, Curiel Yuste, J, Don, A, Epron, D, Formanek, P, Franzluebbers, A, Ilstedt, U, Kätterer, T, Orchard, V, Reichstein, M, Rey, A, Ruamps, L, Subke, J A, Thomsen, I K, Chenu, C, 2012. The moisture response of soil heterotrophic respiration: interaction with soil properties. Biogeosciences 9, 1173–1182.

Nguyen, N H, Song, Z, Bates, S T, Branco, S, Tedersoo, L, Menke, J, Schilling, J S, Kennedy, P G, 2016. FUNGuild: an open annotation tool for parsing fungal community datasets by ecological guild. Fungal Ecology 20, 241–248.

Oksanen, J, Blanchet, F G, Friendly, M, Kindt, R, Legendre, P, McGlinn, D, Minchin, P R, O'Hara, R B, Simpson, G L, Solymos, P, Stevens, M H, Szoecs, E, Wagner, E, 2019. Vegan: Community Ecology Package. R package version 2.5-4.

Parada, A E, Needham, D M, Fuhrman, J A, 2016. Every base matters: assessing small subunit rRNA primers for marine microbiomes with mock communities, time series and global field samples. Environmental Microbiology 18, 1403–1414.

Parton, W J, Schimel, D S, Cole, C V, Ojima, D S, 1987. Analysis of factors controlling soil organic matter levels in great plains grasslands. Soil Science Society of America Journal 51, 1173–1179.

Paustian, K, Parton, W J, Persson, J, 1992. Modeling soil organic matter in organic-amended and nitrogen-fertilized long-term plots. Soil Science Society of America Journal 56, 476–488.

Piccolo, M C, Neill, C, Cerri, C C, 1994. Net nitrogen mineralization and net nitrification along a tropical forest-to-pasture chronosequence. Plant and Soil 162, 61–70.

Pinheiro, J, Bates, D, DebRoy, S, Sarkar, D, R Core Team, 2017. Nlme: linear and nonlinear mixed effects models. R package version 3, 1–131.

Pulido, F, Picardo, A, Campos, P, Carranza, J, Coleto, J, Díaz, M, Diéguez, E, Escudero, A, Ezquerra, F, Fernández, P, Solla, A, 2010. Libro Verde de la Dehesa. Junta de Castilla y León, SECF, SEEP, AEET, SEO, Spain.

R Core Team, 2016. R: A Language and Environment for Statistical Computing. R Foundation for Statistical Computing, Vienna, Austria.

Reichstein, M, Bahn, M, Ciais, P, Frank, D, Mahecha, M D, Seneviratne, S I, Zscheischler, J, Beer, C, Buchmann, N, Frank, D C, Papale, D, Rammig, A, Smith, P, Thonicke, K, van der Velde, M, Vicca, S, Walz, A, Wattenbach, M, 2013. Climate extremes and the carbon cycle. Nature 500, 287–295.

Rodríguez, A, Curiel Yuste, J, Rey, A, Durán, J, García-Camacho, R, Gallardo, A, Valladares, F, 2017. Holm oak decline triggers changes in plant succession and microbial communities, with implications for ecosystem C and N cycling. Plant and Soil 414, 247–263.

Rodríguez, A, Durán, J, Rey, A, Boudouris, I, Valladares, F, Gallardo, A, Curiel Yuste, J, 2019. Interactive effects of forest die-off and drying-rewetting cycles on C and N mineralization. Geoderma 333, 81–89.

Sardans, J, Peñuelas, J, 2005. Drought decreases soil enzyme activity in a Mediterranean *Quercus ilex* L. forest. Soil Biology and Biochemistry 37, 455–461.

Sardans, J, Peñuelas, J, 2013. Plant-soil interactions in Mediterranean forest and shrublands: impacts of climatic change. Plant and Soil 365, 1–33.

Schlesinger, W H, Rhoades, C C, Vose, J M, Rustad, L E, Dietze, M C, Phillips, R P, Jackson, R B, 2016. Forest biogeochemistry in response to drought. Global Change Biology 22, 2318–2328.

Schmidt, P-A, Bálint, M, Greshake, B, Bandow, C, Römbke, J, Schmitt, I, 2013. Illumina metabarcoding of a soil fungal community. Soil Biology and Biochemistry 65, 128–132.

Spieck, E, Bock, E, 2015. Nitrospira. In: Whitman, W B, Rainey, F, Kämpfer, P, Trujillo, M, Chun, J, DeVos, P, Hedlund, B, Dedysh, S (Eds.), Bergey's Manual of Systematics of Archaea and Bacteria New York, NY.

Stark, C H, Richards, K G, 2008. The continuing challenge of nitrogen loss to the environment: environmental consequences and mitigation strategies. Dynamic Soil, Dynamic Plant 2, 41–55.

Tuomi, M, Rasinmäki, J, Repo, A, Vanhala, P, Liski, J, 2011. Soil carbon model Yasso07 graphical user interface. Environmental Modelling & Software 26, 1358–1362.

Valencia, E, Gross, N, Quero, J L, Carmona, C P, Ochoa, V, Gozalo, B, Delgado-Baquerizo, M, Dumack, K, Hamonts, K, Singh, B K, Bonkowski, M, Maestre, F T, 2018. Cascading effects from plants to soil microorganisms explain how plant species richness and simulated climate change affect soil multifunctionality. Global Change Biology 24, 5642–5654.

Vargas, R, Sánchez-Cañete, E, Serrano-Ortiz, P, Curiel Yuste, J, Domingo, F, López-Ballesteros, A, Oyonarte, C, 2018. Hot-moments of soil CO_2 efflux in a water-limited grassland. Soil Systems 2, 47.

Vilà, M, Sardans, J, 1999. Plant competition in mediterranean-type vegetation. Journal of Vegetation Science 10, 281–294.
Wang, S, Chen, Y, 2018. Phylogenomic analysis demonstrates a pattern of rare and long-lasting concerted evolution in prokaryotes. Communications Biology 1, 12.
Xu, Z, Jiang, Y, Zhou, G, 2016. Nitrogen cycles in terrestrial ecosystems: climate change impacts and mitigation. Environmental Reviews 24, 132–143.
Zuur, A F, Ieno, E N, Elphick, C S, 2010. A protocol for data exploration to avoid common statistical problems. Methods in Ecology and Evolution 1, 3–14.